The circadian system throughout the seasons of life

Buijink, M.R.

Chapter 8

Loss of temporal coherence in the aging circadian system: A metabolomics approach.

M. Renate Buijink, Michel van Weeghel, Laura Kervezee, Alida Kindt, Amy Harms, Devika S. Murli, Johanna H. Meijer, Thomas Hankemeier, Stephan Michel

Abstract

Aging is associated with an accumulation of disruptions in metabolic processes, most of which are known to follow a circadian rhythm. Disturbances in circadian rhythms in the metabolic system are related to multiple aging-associated diseases, like diabetes type 2 and neurodegenerative diseases whereas a well-functioning circadian clock is believed to slow down the development of these disorders. Therefore, gaining insight in healthy 24-hour rhythms, and the interactions in biochemical processes, as well as how these alter during aging could benefit the development of strategies to promote healthy aging. Here, we applied multi-tissue metabolomics to obtain a system-wide view on 24-hour rhythmicity, in young and aged mice. We found that in the periphery, a large portion of metabolites showed 24-hour oscillations in young mice. In the liver of old mice, 60% of these metabolites lost their rhythmicity, while this was the case for only a fraction of metabolites in plasma. In the central circadian clock, the suprachiasmatic nucleus (SCN), we observed an increased rhythmicity of metabolites with aging. Interestingly, we found strong correlations in metabolite levels between the liver and plasma, and between the SCN and the paraventricular nucleus of the hypothalamus (PVN) in young mice. However, in old mice, these connections were almost completely abolished. These results indicate that aging is accompanied by a severe loss of the coordination between tissues and disturbed rhythmicity of metabolic processes.

1. Introduction

Life expectancy in Europe has risen by more than 15 years since the 1950s (Roser, 2013). Unfortunately, the last years of life often come with a debilitating decline of bodily functions. One of the affected functions, even in healthy aging, are the daily rhythms in many physiological processes, like sleep and metabolism (Panagiotou *et al.*, 2017; Sato *et al.*, 2017). This results in temporal misalignment, a discrepancy in the phases of different processes, like increased renal activity during nighttime (Schmitt *et al.*, 2019). Circadian misalignment can occur both within a cell or tissue, as well as between different organs, and contributes to aging-associated diseased states, like inflammation, atherosclerosis, obesity, type 2 diabetes and Parkinson's as well as Alzheimer's disease (Castanon-Cervantes *et al.*, 2010; Leng *et al.*, 2019; Schilperoort *et al.*, 2020). This underscores the importance of maintaining, and when possible, strengthening circadian rhythms in the elderly (Buijink & Michel, 2021).

The circadian clock and the aging process are tightly connected to metabolism (Welz & Benitah, 2020). The circadian system has evolved to make optimal use of daily cycles, primarily in food availability (Gerhart-Hines & Lazar, 2015). By timing the activation of molecular systems just before anticipated energy intake and usage, as well as systems for reducing damage by harmful side effects from energy production (e.g., reactive oxygen species (ROS)), and timing repair and maintenance work in the resting phase (when energy intake is unlikely), an organism makes optimal use of energy availability against minimal costs (Asher & Schibler, 2011; Panda, 2016). When the timing of these processes is off, this will lead to increased chances of damage to intracellular molecules, like proteins and DNA, which in turn yield dysfunctional cells (Koritala *et al.*, 2021). The cellular protection and repair mechanisms are not entirely flawless, and the accumulation of damage to the DNA and other subcellular structures is considered to be a central cause of the aging process (López-Otín *et al.*, 2013). Given its role in protecting against these harmful processes, the functioning of the circadian clock is expected to be correlated to the speed at which the aging process takes place (Kondratov *et al.*, 2006; Dubrovsky *et al.*, 2010). It is an appealing idea that the aging process can be slowed down – or at least stirred towards "healthy aging" - by strengthening the clock. However, we need more insight into the causal relationship between aging and the circadian clock function to be able to identify potential targets for successful interventions.

Aging does not affect all levels of the circadian clock in the same way, and some parts are clearly more impaired than others (Buijink & Michel, 2021). For instance, the molecular clock within SCN neurons seems largely unaffected in aging (Kolker *et al.*, 2003; Buijink *et al.*, 2020), while the cell cytosol (e.g. calcium), and membrane elements of the clock, as well as the amplitude of the rhythm in action potential frequency are severely affected

(Nakamura *et al.*, 2011; Farajnia *et al.*, 2012). It remains challenging to thoroughly study the relationship between the aging processes and the circadian clock, given the complex interactions between many levels of the clock, from molecular to behavior (Buijink & Michel, 2021). Omics-studies, like genomics and transcriptomics offer a way to gain more insights on a systemic level (Zierer *et al.*, 2015). Given that metabolic processes are highly interconnected with the circadian system, we have aimed to investigate the circadian rhythms with the use of metabolomics.

Metabolomics offers a comprehensive view the biochemical state of the investigated biological sample. Further development of more efficient high-throughput metabolomics methods, such as in the field of mass spectrometry, have made it more suitable to circadian rhythms studies that typically involve relatively large sample sets due to their longitudinal design. This led to the exciting development of diagnostic and biomarker tools, for example to accurately determining body time from just one sample (Minami *et al.*, 2009; Kasukawa *et al.*, 2012; Cogswell *et al.*, 2021). In addition, metabolomics studies have also shown the influence of environment and behavior on the function of the circadian system. A high-fat diet has been shown to significantly affect metabolite rhythms in the liver and reduce the temporal relationship of metabolites between different tissues in mice (Eckel-Mahan & Sassone-Corsi, 2013; Dyar *et al.*, 2018). Metabolomics have been widely used to study the aging process (Srivastava, 2019), however, the incorporation of the circadian rhythms in the metabolome is unique to the present study. Knowledge on how metabolite levels fluctuate during the day, and how these rhythms change during aging can contribute to the development of targeted interventions and diagnostic tools for age-related diseases.

In the present study we assessed the temporal regulation of biochemical processes, how these processes relate to one another between organs, and how these are affected in aging. We first assessed the rhythmicity of metabolite profiles in the SCN, PVN, plasma and liver. Subsequently, we mapped how metabolite rhythms and levels associate between these tissues. Finally, we addressed how aging affects these metabolite profiles and their mutual coherence. We found that many metabolites show daily rhythms in metabolite levels and that aging severely affects the amplitude or phase of these daily fluctuations, especially in the liver. In all tissues, many of the measured metabolites are found at significantly different levels in tissue from old, compared to young mice. In young mice, there was a clear correlation between the metabolic profile of the SCN and PVN, and between the liver and plasma, which was almost completely lost in aging. We conclude that aging severely affects metabolite level, rhythmicity and systemic temporal coherence.

2. Method

2.1 Animals and housing

Male C57BL/6 mice were kept at the animal facility of the Leiden University Medical Center. The mice were held under a light-dark cycles with 12 hours of light (150-200 lux; Osram truelight TL) and 12 hours of darkness, with food and water were provided at libitum. The study was performed in accordance with the Dutch law on animal welfare, with a permit from the animal experiments committee Leiden (DEC 12250).

2.2 Tissue sampling

C57BL6 mice were sacrificed by decapitation at ZT 2, 6, 10, 14, 18 and 22 (Fig.1A). Young mice were two months old and old mice were between 22 and 25 months old at the time of sacrifice. The liver was dissected, placed in a tube, snapfrozen in liquid nitrogen and stored at -80 °C until further processing (Fig.1B). Trunk blood was collected immediately after decapitation and transferred to a blood collection tube with EDTA (Fig. 1B). The blood samples were kept cold before centrifuging at 5000 rpm for 10 minutes. Plasma was then separated from the pellet, snap frozen and stored at -80 °C until further processing.

SCN and PVN tissue was collected as described earlier (Fig. 1B; (Buijink *et al.*, 2018). In short, the brain was kept in ice cold, low Ca^{2+} and high Mg^{2+} artificial cerebral spinal fluid (ACSF), containing (in mM): NaCl (116.4), KCl (5.4), NaH_2PO_4 (1.0), $MgSO_4$ (0.8), $CaCl_2$ (1.0), $MgCl_2$ (4.0), $NaHCO_3$ (23.8), D-glucose (15.1) and 5 mg/L gentamicin (Sigma Aldrich) saturated with 95% O_2 - 5% CO_2 (pH 7.4), while two consecutive coronal slices of 250 µm were cut with a VT 1000S vibratome (Leica). From these slices, bilateral punches of Ø 500 µm (sample corer, 19-gauge, Fine Science Tools) of both the SCN and PVN were collected. The 4 punches, with a total volume of 0,2 mm^3, were placed in 100 µL ice cold 50/50 methanol/H_2O containing 5 µM of internal standards (succinic acid-D4, $^{13}C_5$-valine, $^{13}C_4$-$^{15}N_2$-asparagine, $^{13}C_5$-glutamine and $^{15}N_2$-UMP), snapfrozen in liquid nitrogen and stored at -80 °C until metabolite extraction.

2.2 Metabolite analysis

Metabolite profiling was performed at the biomedical metabolomics facility of the Leiden University (Leiden, The Netherlands). All samples were analyzed on a platform covering 74 amino acids and biogenic amines.

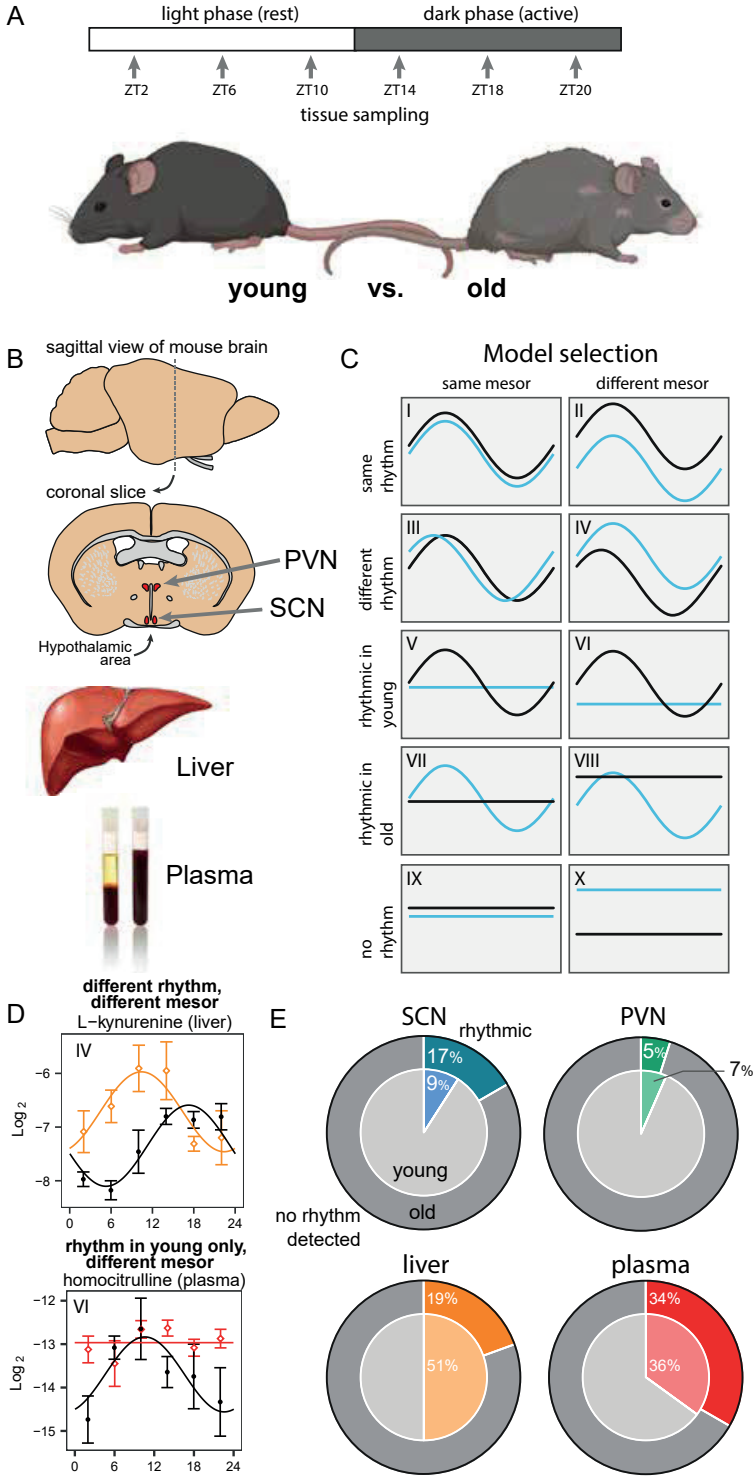
A
light phase (rest)
dark phase (active)
ZT2
ZT6
ZT10
ZT14
ZT18
ZT20
tissue sampling
young vs. old
B
sagittal view of mouse brain
coronal slice
PVN
SCN
Hypothalamic area
Liver
Plasma
C
Model selection
same mesor
different mesor
same rhythm
different rhythm
rhythmic in young
rhythmic in old
no rhythm
I
II
III
IV
V
VI
VII
VIII
IX
X
D
different rhythm, different mesor
L−kynurenine (liver)
IV
Log 2
rhythm in young only, different mesor
homocitrulline (plasma)
VI
E
SCN
rhythmic
17%
9%
young
old
no rhythm detected
PVN
5%
7%
liver
19%
51%
plasma
34%
36%

Figure 1. Assessing 24-hour metabolite profiles in tissues of young and old mice. A) Samples from young and old mice were taken at six time points during the light-dark cycle. B) mice were dissected and SCN, PVN liver and plasma tissues were sampled and processed for LC-MS. C) After data pre-processing, a model-selection approach was used to determine rhythmicity and compare metabolite rhythmicity and level in young and old mice. This results in ten possible outcomes, which are schematically represented. D) Representative examples from the liver (top panel) and plasma (bottom panel) with the black and colored diamonds giving average normalized metabolite level with SEM for young and old, respectively. The solid line represents the sinus or linear fit as selected by the model selection approach. E) The percentage rhythmic metabolites per tissue is given in color, with the inner light-grey ring representing rhythmicity in young mice, and the outer, dark-grey ring in old mice.

2.3 Metabolite extraction

SCN and PVN samples were processed for metabolite extraction as described before (Buijink *et al.*, 2018). In short, 100 µL of chloroform was added to the samples in methanol-water. Then, samples were vortexed, sonicated for 10 minute (while keeping the samples cold) and snapfrozen in liquid nitrogen, which was repeated three times. Proteins were removed by centrifuging the samples for 10 minutes at 14.000 g at 4 °C. 80 µL of the 100 µL polar top layer was transferred to a 1.5 mL tube. Samples were dried for 3 hours in a vacuum concentrator (Labconco, MO, USA).

Liver tissue was freeze dried and pulverized. Around 3 mg of dried liver tissue was weighed and placed in 2 ml tubes. Then, 500 µl of methanol-water (50:50 v/v) with internal standards was added to the sample. For the liquid-liquid extraction, 500 µl of chloroform was added to the samples. For further tissue disruption a Next advance bullet blender 24 was used (2 times for 2 min at intensity 7), with two 3.2 mm steel beads (Next Advance, NY, USA) in the sample. Samples were centrifuged at 16.100 g at 4 °C and 400 µl from the top layer of methanol-water was transferred to a 1.5 mL tube and dried in a vacuum concentrator (Labconco, MO, USA).

Plasma was processed for metabolite extraction by adding 30 µl of H_2O with internal standards and 75 µl of Methanol to 5 µl of plasma. The samples were vortexed and centrifuged for protein precipitation. 105 µl of the top layer was transferred to a clean tube Taken to dryness in a speedvac.

2.4 Derivatization

Metabolites in the SCN, PVN, liver and plasma samples were analyzed by liquid chromatography and mass spectrometry (LC-MS/MS). The dried extracts from SCN, PVN, liver and plasma samples were reconstituted in borate buffer (SCN and PVN: 10 µl, Liver and plasma: 70 µl; pH 8.5), then vortexed for 10 seconds and derivatized with AccQ-TagAQC reagent (SCN and PVN: 2.5 µl, Liver and plasma: 20 µl; Waters). After incubation

at 55 °C for 30 minutes, 20% formic acid (SCN and PVN: 5 µl, Liver and plasma: 10 µl) was added and the samples transferred to a sample vial. Vials were placed in the autosampler tray where they were kept at 4 °C until injection.

2.5 LC-MS/MS

1 µl of the sample was injected onto an Agilent 1290 Infinity II LC System, on an AccQ-Tag Ultra column (Waters) with a flowrate of 0.7 mL/min over an 11 min gradient. The system was coupled to a triple quadrupole mass spectrometer (AB SCIEX Qtrap 6500, Framingham, MA USA). Analytes were detected in the positive ion mode and monitored in Multiple Reaction Monitoring (MRM) using nominal mass resolution. Data was processed using MultiQuant Software for Quantitative Analysis (AB SCIEX, Version 3.0.2). Samples were measured in random order. The integration of assigned SRM peaks was performed using Quanlynx software (Waters). Peak area was normalized by an internal standard, with $^{13}C^{15}N$-labeled analogues for amino-acids, and closest-eluting labelled amino acids for the other amines.

2.6 Data processing

First, data quality was examined. Peak areas that were below three times the peak area of the blank samples were considered to be below the limit of detection (LOD). If more than 20% of the samples were below the LOD for a given metabolite, that metabolite was excluded for further analysis. Remaining peak areas were divided by the peak areas of the internal standard. The liver samples were normalized to their sample weight. The data was then log2-tranformed. Data points that were more than 3 times the standard deviation from the mean of that metabolite were considered to be outliers, and removed. If more than 20% of the results from one sample met this criterium, the whole sample was considered to be compromised, and removed.

2.7 Data analysis

To compare 24-h rhythms in metabolite profiles in young and old mice, differential rhythmicity analysis was performed in R (v. 4.0.2) as described previously (Atger *et al.*, 2015; Kervezee *et al.*, 2018). In short, a model selection approach was applied on log2 to each metabolite from each tissue in which the fit of different linearized cosinor models was compared using the Bayesian Information Criterion (BIC) to select the optimal model among the set of models. This set comprised ten models (visualized in Figure 1C): (model i, ii) a 24-h rhythm in young and old mice with shared cosinor parameters (i.e. similar amplitude and phase), (iii, iv) a 24-h rhythm in young and old mice with different cosinor parameters (i.e. different amplitude and/or phase), (v, vi) a 24-h rhythm in young mice but not in old, (vii, iix) a 24-h rhythm in old mice but not in young, (ix, x) no 24-h rhythm in old and young mice, assuming a shared mesor between young and old mice (i.e. similar overall levels; model i, iii, v, vii, ix) or a different mesor (i.e. higher or lower overall levels;

model ii, iv, vi, iix, x). The fit of the selected model was compared to the null model (model ix) using a log-likelihood ratio test to assess significance (see Fig. 1D for examples of fits for rhythm and phase). Resulting p-values were corrected for multiple testing using the Benjamini Hochberg method at the tissue-level (FDR < 0.05).

Relations between metabolites within and between tissues were quantified with Pearson correlations coefficient and visualized using Matlab R2018. The circular plot was constructed in Matlab (Kassebaum, 2021). Correlations within and between tissues (Fig. 5) were considered relevant when -0.7 < rho > 0.7. The metabolic profiles of Dyar et al., (2018) and our own study were compared by using a two-way ANOVA on Z-scores of the metabolite levels over time. Since the sampling times in both studies were different (ZT 0, 4, 8, 12, 16, 20, 24 for Dyar et al., (2018) and ZT 2, 6, 10, 14, 18, 22 in the present study), one hour was added to the ZT from Dyar et al., (2018) and one hour subtracted from the ZT of our own study. The last datapoint, ZT 24 was left out of the comparison. A significant interaction ($p < 0.05$) indicates a different 24-hour metabolite profile.

3. Results

3.1 Model selection

The model selection approach was used to assign metabolites into different categories (table 1 and 2). Across tissues and metabolites, all selected models provided a significantly better fit than the null model (model IX in Figure 1C; all corrected p-values < 0.05).

3.1 Metabolite rhythms and levels in SCN and PVN

For a small number of metabolites in the SCN and PVN we detected a daily rhythm in their levels (Fig. 1E). In total 9% (n = 6) of the measured metabolites (n = 66) were rhythmic in the SCN in young and 17% (n = 11) in old, with 5 being rhythmic in both young and old (Fig. 2A). Peak time was similar in young and old SCN, with 3 out of 5 metabolites peaking between ZT18 and ZT20 in young and 10 out of 11 in old (Fig. 2B). A list of metabolites per model for the SCN is given in table 1 and examples for every model selection for the SCN is given in figure 2C. In the PVN, 7% (4) of the measured metabolites (n = 61) were found to be rhythmic in young, and 5% (n = 3) in old, with only 2 metabolites being rhythmic in both young and old (Fig. 2C). Peak times were dispersed in both young and old PVN tissue (Fig. 2E). We did find a difference in metabolite levels between young and old SCN and PVN tissue (Fig. 2A & 2B). In total 57% (n = 37) of metabolites in the SCN (Fig. 2A), and 74% (n = 45) of metabolites in the PVN (Fig. 2B) showed a significantly different level in tissue from old, compared to young mice. A list of metabolites per model for the PVN is given in table 1 and examples for every model selection for the PVN is given in figure 2F.

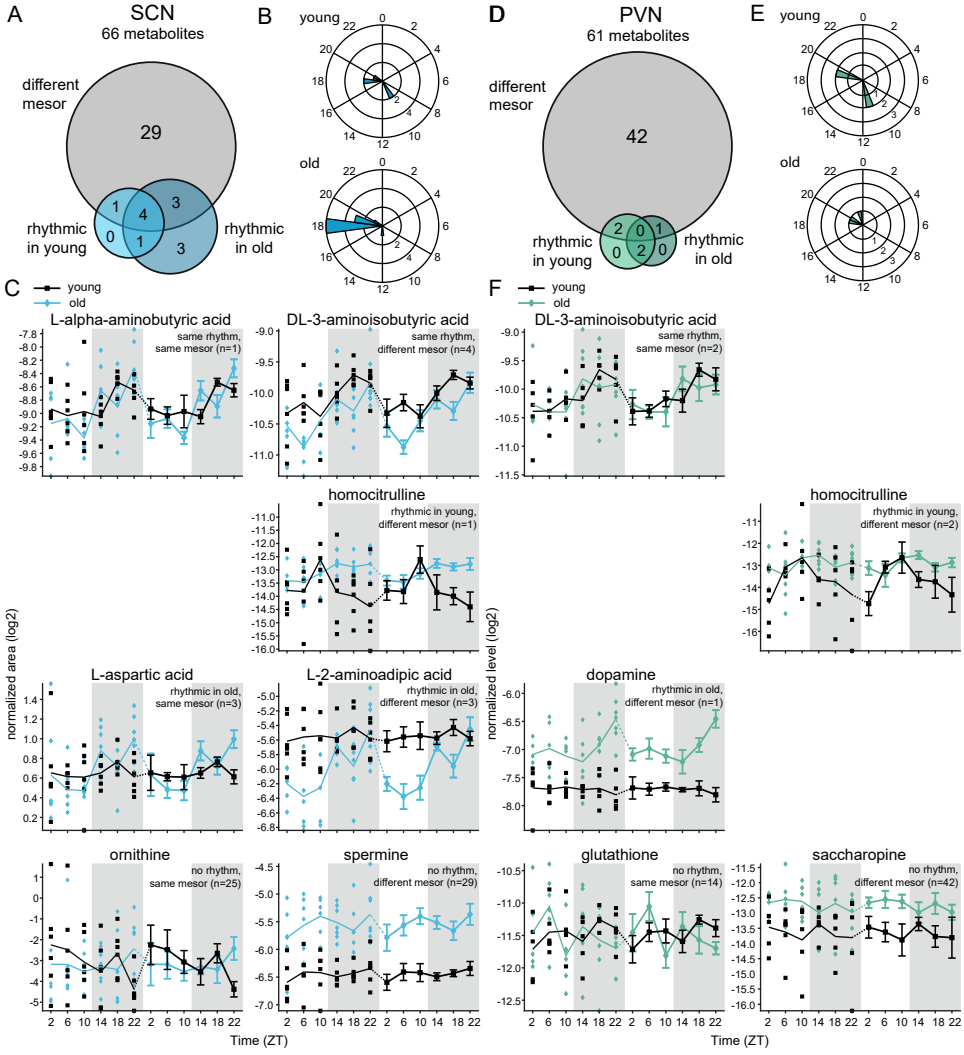

Figure 2. Assessing 24-hour metabolite profiles in tissues of young and old mice. A) Samples from young and old mice were taken at six time points during the light-dark cycle. B) mice were dissected and SCN, PVN liver and plasma tissues were sampled and processed for LC-MS. C) After data pre-processing, a model-selection approach was used to determine rhythmicity and compare metabolite rhythmicity and level in young and old mice. This results in ten possible outcomes, which are schematically represented. D) Representative examples from the liver (top panel) and plasma (bottom panel) with the black and colored diamonds giving average normalized metabolite level with SEM for young and old, respectively. The solid line represents the sinus or linear fit as selected by the model selection approach. E) The percentage rhythmic metabolites per tissue is given in color, with the inner light-grey ring representing rhythmicity in young mice, and the outer, dark-grey ring in old mice.

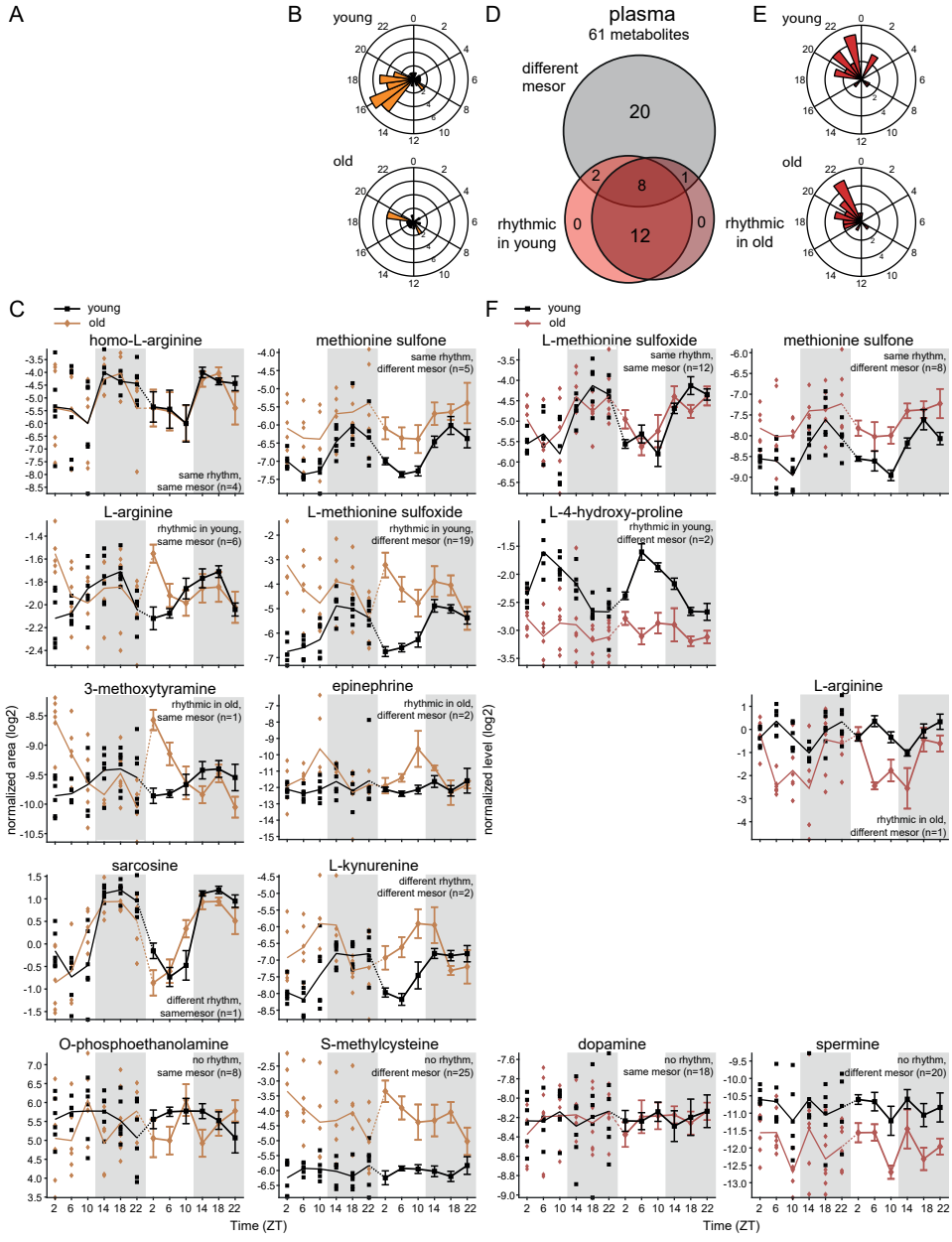

Figure 3. Metabolite rhythms and levels change in liver and plasma in the course of aging. The number of metabolites that change level (grey circle) and/or are rhythmic (color circles) in young, in old, or in both are given for the liver (A) and plasma (D). Phase plots give the peak time of the rhythmic metabolites in young (top panel) and old (bottom panel) in the liver (B) and plasma (E). Representative double-plotted examples of the selected models, based on changes in average levels, represented by mesor and rhythmicity, determined with sinus fitting shown for the liver (C) and plasma (F). Metabolite levels are represented in the log2 of the MS peak area divided by the

internal standard. The first part or the double-plot shows the individual data points and their mean over time (solid line). Mean levels and SEM over time are represented in the second part. Grey areas mark dark period (active phase) and light areas represent time of lights-on (inactive phase). For plasma, models IV, V, VII and VIII were not observed.

3.2 Metabolite rhythms and levels in the liver and plasma

In the liver of young mice, 51% (n = 37) of all measurable metabolites (n = 73) showed a daily rhythm in their level (Fig. 1E). This percentage was largely reduced in aging, where only about 21% (n = 15) showed a rhythm, with 12 metabolites being rhythmic in both young and old (Fig. 3A). Most metabolites in the liver peak in the night in both young and old mice, between ZT12 and ZT 24 (n = 29/37 in young and n = 11/15 in old; Fig. 3B). However, in young mice, there is a clear peak at ZT16 that is absent in old mice. A list of metabolites per model for the liver is given in table 2 and examples for every model selection for the liver is given in figure 3C. In plasma, 36% (n = 22) of the measured metabolites (n = 61) showed a rhythm, and most metabolites remained rhythmic in aging, 34% (n = 21) was rhythmic in aging, with 20 metabolites being rhythmic in both young and old (Fig. 3D). In both young and old mice, the majority of metabolites peak between ZT17 and ZT24 (n = 16/22 in young and n = 19/21; Fig. 3E). However, in young mice, the peak times are more consolidated between ZT18 and ZT23) As in the SCN and PVN, many metabolites were either higher or lower in the liver and plasma from old, compared to young mice (Fig. 3A and 3D). 72% (n = 52) of metabolites in the liver, and 51% (n = 30) of metabolites in plasma show a different level in aging. A list of metabolites per model for plasma is given in table 2 and examples for every model selection for the plasma is given in figure 3F.

3.3 Correlations between metabolites within tissues

We next sought to find to what extend metabolites correlate within the examined tissues (Fig. 4). Correlations were considered of interest when -0.7 < rho > 0.7. Between 7.5% and 15% of the correlations met this criterium in tissue of young mice. In aging, the number of correlations increased in all tissues (Fig 4E). The largest increase was noticeable in the liver, where 487 combinations of metabolites correlated with rho < -0.7, or rho > 0.7 in young, versus 713 in old liver tissue.

3.4 Correlations of metabolite levels between tissues

The four collected tissues originated from individual animals, making it possible to correlate the metabolite levels between the investigated tissues (Fig. 5). Per metabolite, levels were compared with all metabolites within and between the 4 tissues, resulting in a correlation matrix of 261x261 (Fig. S 2). It is clear that the correlations between metabolites

within tissues are higher than between tissues. It also shows that higher correlations are exclusively found between the SCN and PVN and between plasma and the liver and that these correlations change in aging. To get more insight in these changes in aging, we constructed a circular graph, depicting correlations with rho > 0.7 (Fig. 5). There are indeed strong connections between the SCN and PVN and between plasma and the liver, while these are completely absent between the brain and peripheral tissues. In old mice, almost all connections are lost (Fig. 5).

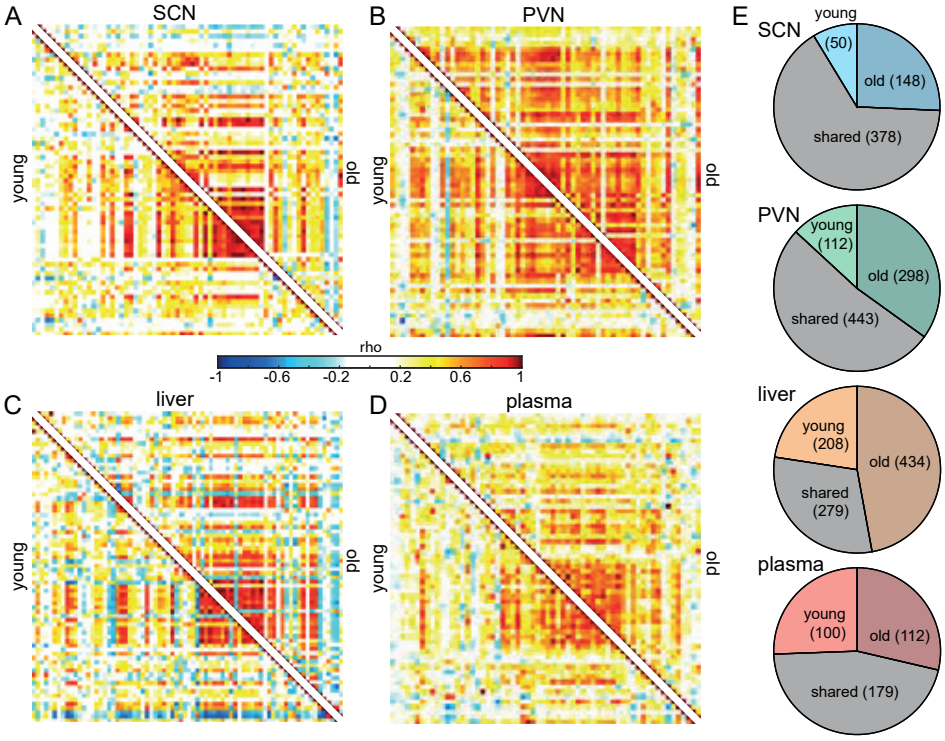

Figure 4. Within-tissue correlations of metabolite levels in SCN, PVN, liver and plasma of young and old mice. Correlation matrices with colours indicating rho values for correlations between metabolites within the SCN (A), PVN (B), liver (C) and plasma (D). Correlations in tissue from young mice are shown in the left-bottom half of the panel, and for old mice in the top-right half. The fraction of metabolites with correlations rho < -0.7 and rho > 0.7 in young, in old, or in both are shown in (E).

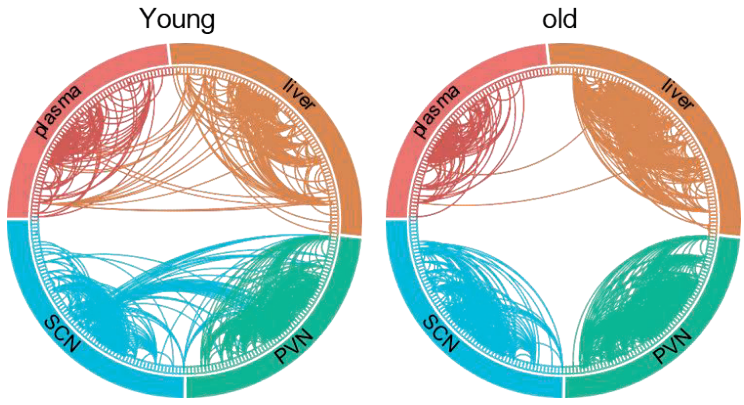

Figure 5. Within and between-tissue correlations of metabolite levels for young and old mice. Lines connect metabolites with strong correlations (rho < -0.7 and rho > 0.7) within and between SCN (blue), PVN (green), liver (orange) and plasma (pink), for young (left panel) and old (right panel).

3.5 Correlations, levels and rhythmicity of alpha-aminobutyric acid and beta-aminoisobutyric acid

When we look into the correlations of individual metabolites between tissues, alpha-aminobutyric acid (AABA) stands out with 8 out of 12 pairs (young vs. old for SCN, PVN, liver and plasma) that are significantly correlated ($p < 0.05$; Fig. 6). Interestingly, together with another aminobutyric acid, beta-aminoisobutyric acid (BAIBA), AABA is one of the only two metabolites rhythmic in both the SCN and PVN, and in both young and old mice (table 1; Fig. 7). In addition, BAIBA is also rhythmic in the liver of young mice (Fig. 7). Unfortunately, BAIBA could not be measured reliably in plasma.

3.6 Generalization of results on metabolite level

To investigate to what extend the results on individual metabolite level can be generalized, we compared our results from the SCN, liver and plasma to the results from Dyar et al., 2018 (Fig. S1). We compared the control groups of these studies, both performed in young C57BL6 mice (6 and 8 weeks old). Interestingly, from the metabolites that were measured in both studies, we found that from the liver 8 out of 31 significantly different. From the profiles of plasma metabolites 3 out of 30 were significantly different. For the metabolites in the SCN, comparison was more difficult, since the SD in both data sets are higher. From the SCN profiles 3 of 31 differed significantly. Additional visual inspection indicates that for the liver and plasma, most profiles that are not significantly different indeed look very similar, while for profiles in the SCN tissue this is less clear.

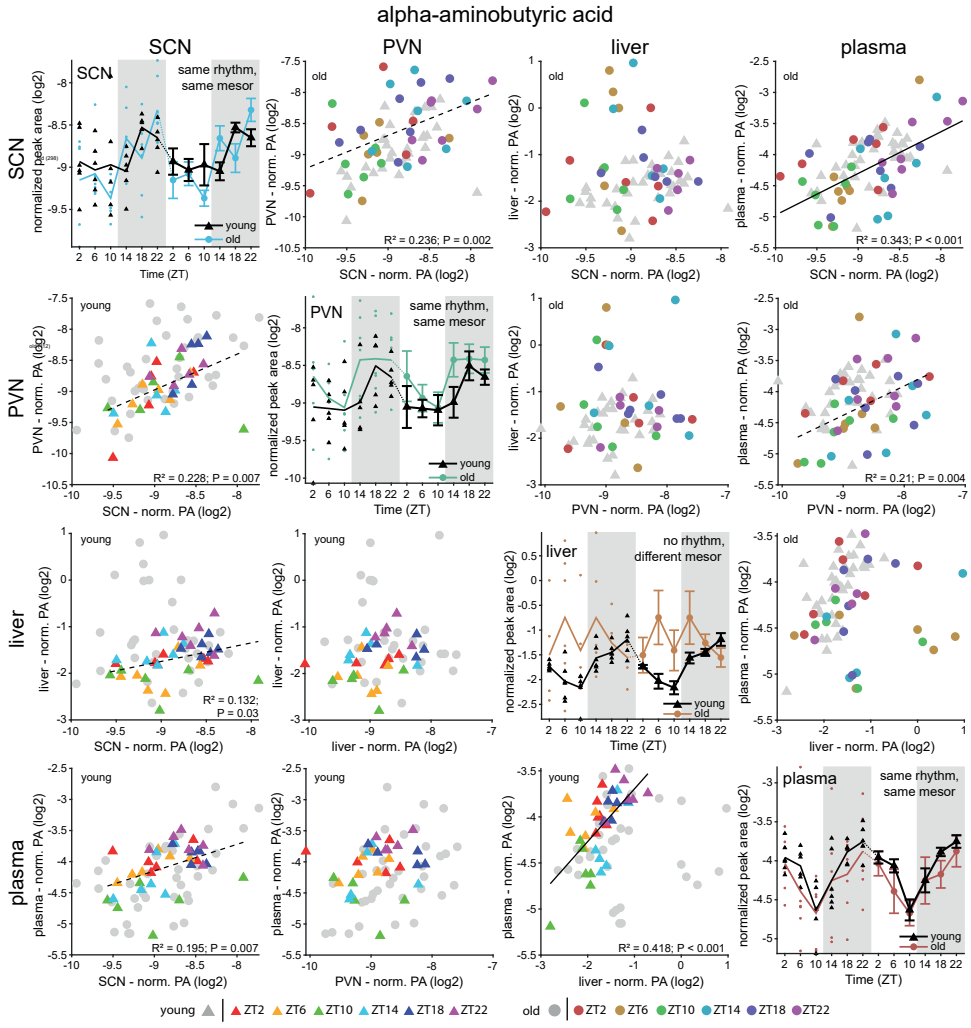

Figure 6. metabolite levels over time per tissue, and correlations between tissues for alpha-aminobutyric acid. Diagonal panels show metabolite levels over time for young (colored) and old (black) in the SCN, PVN, liver and plasma. Metabolite levels are represented in the log2 of the MS peak area divided by that of the internal standard. The first part or the double-plot shows the individual data points and their mean over time (solid line). Mean levels and their standard deviations over time are represented in the second part. Grey areas mark dark period (active phase) and light areas represent time of lights-on (inactive phase). The six left-bottom panels represent correlations between the tissues, with values in young mice in color, and for old mice in grey; the right-top six panels give values for old mice in color and for young mice in grey. Colors code for zeitgeber time (ZT; ZT2 = red, ZT6 = yellow, ZT 10 = green, ZT 14 = blue, ZT 18 = purple and ZT22 = pink). Significant correlations are indicated by either a dotted line ($0.0001 < P < 0.05$, or by solid line ($P < 0.001$).

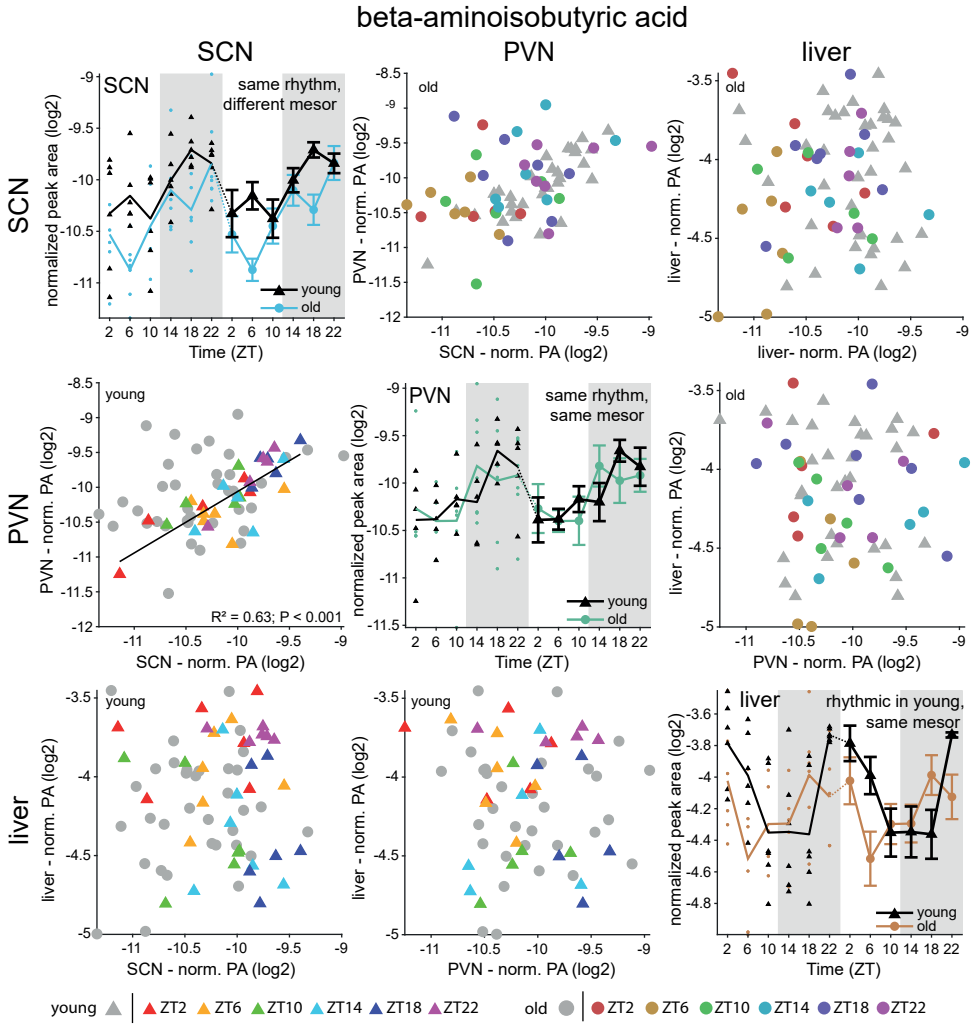

Figure 7. metabolite levels over time per tissue, and correlations between tissues for beta-aminoisobutyric acid. See legend figure 6. In plasma, beta-aminoisobutyric acid levels were below the limit of detection.

4. Discussion

We used metabolomic analysis of brain and peripheral tissues, collected at different timepoints, to assess temporal regulation of metabolites within and between different tissues in young and old mice. We show that 24-hour rhythms in metabolite levels are most abundant in the liver, with 50% of the measured metabolites showing rhythmicity in their levels. However, we found a notable reduction of 60% in rhythmicity of liver metabolites in

aging. By contrast, in plasma, about one third of metabolites are rhythmic, and almost all of these remain rhythmic in old mice. In the SCN and PVN, the percentage of metabolites that was found to be rhythmic was lower (7-10%), however, the rhythmic fraction almost doubled in the aged SCN (to 17%). Analysis of the correlation between metabolite levels in the collected tissues show a clear link between metabolite dynamics in the SCN and PVN, and between the liver and plasma. This relationship is almost completely lost in aging. These results indicate that metabolite levels are regulated between the SCN and PVN and between liver and plasma. The loss of the coherence in aging indicates disturbed communication between these tissues, which will have system-wide consequences.

4.1 Rhythmicity of metabolites in brain and periphery

In the SCN and PVN of young mice 9% and 7% of the detected metabolites showed a 24-hour rhythm, respectively. This is similar to the results from Dyar et al. (2018), showing rhythmicity in about 12% of the measured metabolites in the SCN of mice on a normal diet. Interestingly, in our study, the percentage of rhythmic metabolites increased markedly in aged mice, which was also the case in the SCN of mice on a high fat diet (Dyar *et al.*, 2018). In both studies there is no obvious explanation for this increase in rhythmic metabolites. A gain in circadian rhythms was also found in a group of genes in the human prefrontal cortex, which was suggested to be the result of a compensatory mechanism for a breakdown of the canonical clock genes (Chen *et al.*, 2016). In our study, most metabolites remained rhythmic in the SCN, and an additional group of metabolites gained rhythmicity, whereas in the previously mentions studies, the gain of rhythmicity was due to a proportion of metabolites losing their 24-hour rhythms, while another, relatively large proportion gained rhythmicity (Chen *et al.*, 2016; Dyar *et al.*, 2018). One intriguing hypothesis to explain gain of rhythmicity in metabolites is that the temporal control of biochemical pathways is reorganized, to compensate for affected processes by e.g., a high fat diet or aging. In the case of a high fat diet, additional analysis of the data from Dyar et al., (2018) showed that, contrary to our results, the amino acids do not gain rhythmicity (Tognini *et al.*, 2020). It remains unclear how this putative reorganization could be established, but the challenging task to understand the mechanisms will give insights into plasticity of intracellular signaling, which will be beneficial to many fields of cellular physiology. The challenge lies in the fact that, there are many interacting processes within and between the different levels of organization within a cell, from genes to metabolites. Furthermore, a single metabolite is involved in a multitude of metabolic pathways, making it difficult to pinpoint changes to a specific process. It will require a well-designed combination of experimental techniques to investigate the causal relationships of the multi-level circadian mechanisms simultaneously. However, it is encouraging that directly comparing our metabolomics results with that of another metabolomics-study (Dyar et al., 2018) show that these results are very similar, which confirms the potential of the combining of metabolomics studies and the valid interpretation of the resulting data.

4.2 Aging affects metabolite levels and rhythmicity in a tissue-specific matter

We found that for many metabolites, levels were altered in the tissues of aged mice, compared to young mice. Most metabolites showed an increased abundance in the aged mice. This is in line with previous reports of metabolomic profiles in aging (Houtkooper *et al.*, 2011; Held *et al.*, 2020). Levels and rhythmicity of metabolites measured in plasma were least affected by aging, with half of the measurable metabolites displaying changed levels in aged, compared to young mice, and only a few metabolites losing rhythmicity. These results are relevant for the assessment of the application of metabolomics to determine circadian phase in humans, since plasma is among the least invasive sample source for diagnostics, and, contrary to saliva, breath, urine, feces and other excretory substances, blood plasma is part of the internal milieu, and central part of the whole-body physiology. However, given our results, it might be more difficult to detect rhythm deficits through the analysis of (amines in) plasma. In the PVN and liver, metabolite levels are most affected by aging, with over 70% of the measured metabolites displaying a different level in old mice. The effect of aging on metabolite profiles in blood plasma and the liver are clearly distinct from diet-induced changes in circadian metabolomics, since in a high fat diet metabolites in the blood are more severely than those in the liver (Dyar *et al.*, 2018). Importantly, the timing of feeding (irrespective of diet) also affects metabolite rhythmicity. For instance, in the liver the phase of metabolite rhythms, but also of the molecular clock genes, readily adapt to reversed feeding rhythms in metabolic tissues, like the liver (Damiola *et al.*, 2000; Xin *et al.*, 2021). Since aging is known to be accompanied by changes in circadian rhythms in activity and feeding (Houtkooper *et al.*, 2011; Buijink *et al.*, 2020), this could account for some of the changes found in the metabolic profile in old mice.

4.3 Convergence of rhythms in Beta-aminoisobutyric acid and alpha-aminobutyric acid between tissues

Metabolomics is a highly effective method to study physiological state and to identify biomarkers. However, it remains a challenge to translate the metabolomics profiles to specific biological processes. Examining specific metabolites that show an interesting pattern or change in response to changed experimental conditions might reveal new insight in their role in biological processes. In the present study we found two metabolites that show such an interesting pattern, namely alpha-aminobutyric acid (AABA) and beta-aminoisobutyric acid (BAIBA).

Within the group of metabolites we studied, AABA and BAIBA are the only two metabolites that showed a clear 24-hour rhythm in both the SCN and PVN, and in young and old mice. Moreover, for BAIBA, levels were highly correlated between the SCN and PVN in young mice, but not in the SCN and PVN from old mice. The correlation seems independent of the similarity in the 24-hour rhythm, since specific timepoints do not cluster together, and the correlation is lost in aging, while the 24-hour rhythm is maintained, and therefore, to

be irrespective of its temporal regulation. Like AABA, BAIBA is a non-proteinergic amino acid that was discovered in human urine, in 1951 (Crumpler et al., 1951). It is the end product of thymine and valine catabolism, with thymine in turn being an intermediate from DNA catabolism. This amino acid has gained interest in recent years, since it was discovered that BAIBA induces the browning of white fat (Roberts *et al.*, 2014). BAIBA acts as a myokine, a molecule that is released from muscle tissue upon muscle contractions, and that serve as an autocrine, paracrine or endocrine factor. BAIBA has been found to be involved in the communication between muscle and bone (Kitase *et al.*, 2018), and could possibly also acts as a signal between muscle and brain. Given the lack of knowledge on the role of BAIBA in the brain, it is difficult to speculate on its role in the SCN and PVN, and its link to the circadian system. However, a recent study has shown that administering BAIBA in the drinking water of mice reduced high-fat diet induced inflammation in the hypothalamus (Park *et al.*, 2019), the brain area where both the SCN and PVN are part of (although these areas were not specifically investigated in the study). This indicates an interesting immunological function for BAIBA in the brain. Given that BAIBA levels are lower in the SCN in aging, there might be a connection to neuroinflammation that is seen in the aging brain (Di Benedetto *et al.*, 2017).

As said, AABA and BAIBA are the only metabolites in our study that are rhythmic in both the SCN and PVN, and in both young and old mice. Moreover, AABA is also rhythmic in plasma, and – although not strong enough to surpass our threshold of rho > 0.7 – there is a significant correlation between all tissues, which can partially be due to the corresponding peak time of AABA in the different tissues (ZT18-ZT22). AABA is a non-proteinergic amino acid that was discovered in urine of patients with hepatic disease after administering methionine (Dent et al., 1946). AABA can serve as a biomarker in blood and urine for several metabolic and hepatic diseases, cancer, Alzheimer's disease and schizophrenia (Fonteh *et al.*, 2007; Cheng *et al.*, 2012; Yang *et al.*, 2013).

The finding that AABA and BAIBA are rhythmic in the SCN and PVN raises the question whether there might be a link between these amino acids and the circadian clock. The biological role of AABA is not well known, and there are to our knowledge no studies on a role for AABA in the brain. For BAIBA there might be a connection to the clock, since BAIBA excretion was stimulated by overexpression of Peroxisome proliferator-activated receptor gamma coactivator 1-alpha (PGC-1α) in myocytes (Roberts *et al.*, 2014). PGC-1α in turn is known to regulate the expression of the core clock genes BMAL1 and CLOCK, and to be itself rhythmically expressed in the liver and muscle (Liu *et al.*, 2007). This does not necessarily mean that this link is direct: the peak in PGC-1α in the liver seems to be in the beginning of the night, while our results indicate that the peak in BAIBA in the liver occurs at the end of the night. Moreover, GABA is also regulated by PGC-1α and does not follow the same pattern as BAIBA. It is currently still unknown how PGC-1α regulates

BIABA expression in muscle tissue. It will be interesting to see what link there might be between BIABA, PGC-1α and the circadian clock.

4.4 Metabolite levels are interrelated between SCN and PVN, as well as between liver and plasma, a connection that is lost in aging

For an organism to function correctly, many processes within and between tissues need to proceed in a coherent fashion. We show that there are strong correlations among metabolite levels *within* the tissues we analyzed. The correlation *between* the tissues reveals a strong association between the two brain areas, the SCN and PVN, as well as between the two peripheral tissues, the liver and plasma. The SCN and PVN are both located lateral of the third ventricle, with the PVN situated dorsally of the SCN, separated only by the subparaventricular zone (sPVZ). The PVN is one of the few brain areas that is directly innervated by the SCN (Buijs *et al.*, 1999; Kalsbeek & Buijs, 2002), a pathway that regulates the rhythmic release of several hormones involved in feeding, behavioral activity and sleep (Buijs *et al.*, 2019). The SCN is connected to the liver through both the sympathetic and parasympathetic nervous system, and regulates plasma glucose release by the liver through innervations of the PVN (Kalsbeek *et al.*, 2004; Kalsbeek *et al.*, 2010). The mutual connections between the liver and plasma are numerous, the liver filters harmful substances from the blood, and releases hormones and other molecules into the bloodstream to regulate energy metabolism and growth (refs?). Since all four tissues are both physically and functionally strongly connected, it is somewhat surprising that the brain areas and the peripheral tissues are so strictly separated. However, it is clear that the metabolites within the tissues with the closest proximity to each other show the highest correlations.

In aging, the correlation between metabolites *within* the examined tissues is largely unaffected, while the correlations *between* the tissues are almost entirely lost. Exposing mice to a high-fat diet has a similar effect on the correlations of metabolite levels between different tissues (Dyar *et al.*, 2018), implying that in both cases, homeostatic regulatory mechanisms are disturbed. The analysis of correlations among metabolites in different tissues does not distinguish between a temporal, or alternative origin, which would be interesting to include in future analyses. Nevertheless, it is likely that enforcing daily rhythms in feeding and fasting, activity and rest, and timely exposure to light and darkness in aging will likely reenforce rhythms in metabolite profiles and be beneficial for the coherence between tissues, thereby improving whole body homeostasis and health.

4.5 Conclusion

There is a growing number of Omics studies on circadian rhythms on different levels. However, studies that combine multiple tissues or their subregions, multiple subcellular levels, from genes to metabolites, are scares. These studies, including the present study,

provide insight in whole-system circadian effects, either on a cellular level (e.g., between transcripts and metabolites), or on an organism level (e.g., between different organs). We show that the concentration of a substantial set of metabolites fluctuate during the day, and that they are strongly correlated between the SCN and PVN in the brain, as well as between the peripheral liver tissue and plasma in young mice. However, since these correlations is almost completely abolished in aging, it seems that the aging process severely affects the homeostatic coordination of metabolic processes between tissues.

References

Asher, G. & Schibler, U. (2011) Crosstalk between components of circadian and metabolic cycles in mammals. *Cell Metababolism*, 13, 125-137.

Atger, F., Gobet, C., Marquis, J., Martin, E., Wang, J., Weger, B., Lefebvre, G., Descombes, P., Naef, F. & Gachon, F. (2015) Circadian and feeding rhythms differentially affect rhythmic mRNA transcription and translation in mouse liver. *Proceedings of the National Academy of Sciences*, 112, E6579-E6588.

Buijink, M.R. & Michel, S. (2021) A multi-level assessment of the bidirectional relationship between aging and the circadian clock. *Journal of Neurochemistry*, 157, 73-94.

Buijink, M.R., Olde Engberink, A.H.O., Wit, C.B., Almog, A., Meijer, J.H., Rohling, J.H.T. & Michel, S. (2020) Aging affects the capacity of photoperiodic adaptation downstream from the central molecular clock. *Journal of biological rhythms*, 35, 167-179.

Buijink, M.R., van Weeghel, M., Gülersönmez, M.C., Harms, A.C., Rohling, J.H.T., Meijer, J.H., Hankemeier, T. & Michel, S. (2018) The influence of neuronal electrical activity on the mammalian central clock metabolome. *Metabolomics*, 14, 122.

Buijs, R., Hermes, M.H.L.J. & Kalsbeek, A. (1999) The suprachiasmatic nucleus—paraventricular nucleus interactions: A bridge to the neuroendocrine and autonomic nervous system. In Urban, I.J.A., Burbach, J.P.H., De Wed, D. (eds) *Progress in Brain Research*. Elsevier, pp. 365-382.

Buijs, R.M., Guzmán Ruiz, M.A., Méndez Hernández, R. & Rodríguez Cortés, B. (2019) The suprachiasmatic nucleus; a responsive clock regulating homeostasis by daily changing the setpoints of physiological parameters. *Autonomic Neuroscience*, 218, 43-50.

Castanon-Cervantes, O., Wu, M., Ehlen, J.C., Paul, K., Gamble, K.L., Johnson, R.L., Besing, R.C., Menaker, M., Gewirtz, A.T. & Davidson, A.J. (2010) Dysregulation of inflammatory responses by chronic circadian disruption. *Journal of Immunology*, 185, 5796-5805.

Chen, C.Y., Logan, R.W., Ma, T., Lewis, D.A., Tseng, G.C., Sibille, E. & McClung, C.A. (2016) Effects of aging on circadian patterns of gene expression in the human prefrontal cortex. *Proceedings of the National Academy of Sciences*, 113, 206-211.

Cheng, Y., Xie, G., Chen, T., Qiu, Y., Zou, X., Zheng, M., Tan, B., Feng, B., Dong, T., He, P., Zhao, L., Zhao, A., Xu, L.X., Zhang, Y. & Jia, W. (2012) Distinct urinary metabolic profile of human colorectal cancer. *Journal of Proteome Research*, 11, 1354-1363.

Cogswell, D., Bisesi, P., Markwald, R.R., Cruickshank-Quinn, C., Quinn, K., McHill, A., Melanson, E.L., Reisdorph, N., Wright, K.P. & Depner, C.M. (2021) Identification of a Preliminary Plasma Metabolome-based Biomarker for Circadian Phase in Humans. *Journal of Biological Rhythms*, 36, 369-383.

Crumpler, H. R., Dent, C. E., Harris, H., & Westall, R. G. (1951). β-Aminoisobutyric acid (α-methyl-β-alanine): a new amino-acid obtained from human urine. *Nature*, 167, 307-308.

Damiola, F., Le Minh, N., Preitner, N., Kornmann, B.t., Fleury-Olela, F. & Schibler, U. (2000) Restricted feeding uncouples circadian oscillators in peripheral tissues from the central pacemaker in the suprachiasmatic nucleus. *Genes & Development*, 14, 2950-2961.

Dent, C. E. (1946). Detection of amino-acids in mine and other fluids. *Lancet*, 251, 637-639.

Di Benedetto, S., Muller, L., Wenger, E., Duzel, S. & Pawelec, G. (2017) Contribution of neuroinflammation and immunity to brain aging and the mitigating effects of physical and cognitive interventions. *Neuroscience & Biobehavioral Reviews*, 75, 114-128.

Dubrovsky, Y.V., Samsa, W.E. & Kondratov, R.V. (2010) Deficiency of circadian protein CLOCK reduces lifespan and increases age-related cataract development in mice. *Aging (Albany NY)*, 2, 936-944.

Dyar, K.A., Lutter, D., Artati, A., Ceglia, N.J., Liu, Y., Armenta, D., Jastroch, M., Schneider, S., de Mateo, S., Cervantes, M., Abbondante, S., Tognini, P., Orozco-Solis, R., Kinouchi, K., Wang, C., Swerdloff, R., Nadeef, S., Masri, S., Magistretti, P., Orlando, V., Borrelli, E., Uhlenhaut, N.H., Baldi, P., Adamski, J., Tschöp, M.H., Eckel-Mahan, K. & Sassone-Corsi, P. (2018) Atlas of Circadian Metabolism Reveals System-wide Coordination and Communication between Clocks. *Cell*, 174, 1571-1585.e1511.

Eckel-Mahan, K. & Sassone-Corsi, P. (2013) Metabolism and the circadian clock converge. *Physiological Reviews*, 93, 107-135.

Farajnia, S., Michel, S., Deboer, T., vanderLeest, H.T., Houben, T., Rohling, J.H., Ramkisoensing, A., Yasenkov, R. & Meijer, J.H. (2012) Evidence for neuronal desynchrony in the aged suprachiasmatic nucleus clock. Journal of Neuroscience *Journal of Neuroscience*, 32, 5891-5899.

Fonteh, A.N., Harrington, R.J., Tsai, A., Liao, P. & Harrington, M.G. (2007) Free amino acid and dipeptide changes in the body fluids from Alzheimer's disease subjects. *Amino Acids*, 32, 213-224.

Gerhart-Hines, Z. & Lazar, M.A. (2015) Circadian Metabolism in the Light of Evolution. *Endocrine Reviews*, 36, 289-304.

Held, N.M., Buijink, M.R., Elfrink, H.L., Kooijman, S., Janssens, G.E., Vaz, F.M., Michel, S., Houtkooper, R.H. & van Weeghel, M. (2021) Aging selectively dampens oscillation of lipid abundance in white and brown adipose tissue. *Scientific Reports* 11, 5932.

Houtkooper, R.H., Argmann, C., Houten, S.M., Cantó, C., Jeninga, E.H., Andreux, P.A., Thomas, C., Doenlen, R., Schoonjans, K. & Auwerx, J. (2011) The metabolic footprint of aging in mice. *Scientific Reports*, 1, 134.

Kalsbeek, A. & Buijs, R.M. (2002) Output pathways of the mammalian suprachiasmatic nucleus: coding circadian time by transmitter selection and specific targeting. *Cell and Tissue Research*, 309, 109-118.

Kalsbeek, A., La Fleur, S., Van Heijningen, C. & Buijs, R.M. (2004) Suprachiasmatic GABAergic Inputs to the Paraventricular Nucleus Control Plasma Glucose Concentrations in the Rat via Sympathetic Innervation of the Liver. *The Journal of Neuroscience*, 24, 7604-7613.

Kalsbeek, A., Yi, C.-X., La Fleur, S.E. & Fliers, E. (2010) The hypothalamic clock and its control of glucose homeostasis. *Trends in Endocrinology & Metabolism*, 21, 402-410.

Kassebaum, P. (2021) CircularGraph. *github.com/paul-kassebaum-mathworks/circularGraph*, Retrieved June 23, 2021.

Kasukawa, T., Sugimoto, M., Hida, A., Minami, Y., Mori, M., Honma, S., Honma, K., Mishima, K., Soga, T. & Ueda, H.R. (2012) Human blood metabolite timetable indicates internal body time. *Proceedings of the National Academy of Sciences*, 109, 15036-15041.

Kervezee, L., Cuesta, M., Cermakian, N. & Boivin, D.B. (2018) Simulated night shift work induces circadian misalignment of the human peripheral blood mononuclear cell transcriptome. *Proceedings of the National Academy of Sciences*, 115, 5540-5545.

Kitase, Y., Vallejo, J.A., Gutheil, W., Vemula, H., Jähn, K., Yi, J., Zhou, J., Brotto, M. & Bonewald, L.F. (2018) β-aminoisobutyric Acid, l-BAIBA, Is a Muscle-Derived Osteocyte Survival Factor. *Cell Reports*, 22, 1531-1544.

Kolker, D.E., Fukuyama, H., Huang, D.S., Takahashi, J.S., Horton, T.H. & Turek, F.W. (2003) Aging alters circadian and light-induced expression of clock genes in golden hamsters. *Journal Of Biological Rhythms*, 18, 159-169.

Kondratov, R.V., Kondratova, A.A., Gorbacheva, V.Y., Vykhovanets, O.V. & Antoch, M.P. (2006) Early aging and age-related pathologies in mice deficient in BMAL1, the core componentof the circadian clock. *Genes & Development*, 20, 1868-1873.

Koritala, B.S.C., Porter, K.I., Arshad, O.A., Gajula, R.P., Mitchell, H.D., Arman, T., Manjanatha, M.G., Teeguarden, J., Van Dongen, H.P.A., McDermott, J.E. & Gaddameedhi, S. (2021) Night shift schedule causes circadian dysregulation of DNA repair genes and elevated DNA damage in humans. *Journal of Pineal Research*, 70, e12726.

Leng, Y., Musiek, E.S., Hu, K., Cappuccio, F.P. & Yaffe, K. (2019) Association between circadian rhythms and neurodegenerative diseases. *The Lancet Neurology*, 18, 307-318.

Liu, C., Li, S., Liu, T., Borjigin, J. & Lin, J.D. (2007) Transcriptional coactivator PGC-1α integrates the mammalian clock and energy metabolism. *Nature*, 447, 477-481.

López-Otín, C., Blasco, M.A., Partridge, L., Serrano, M. & Kroemer, G. (2013) The Hallmarks of Aging. *Cell*, 153, 1194-1217.

Minami, Y., Kasukawa, T., Kakazu, Y., Iigo, M., Sugimoto, M., Ikeda, S., Yasui, A., van der Horst, G.T.J., Soga, T. & Ueda, H.R. (2009) Measurement of internal body time by blood metabolomics. *Proceedings of the National Academy of Sciences*, 106, 9890-9895.

Nakamura, T.J., Nakamura, W., Yamazaki, S., Kudo, T., Cutler, T., Colwell, C.S. & Block, G.D. (2011) Age-related decline in circadian output. *Journal of Neuroscience*, 31, 10201-10205.

Panagiotou, M., Vyazovskiy, V.V., Meijer, J.H. & Deboer, T. (2017) Differences in electroencephalographic non-rapid-eye movement sleep slow-wave characteristics between young and old mice. *Scientific Reports*, 7, 43656.

Panda, S. (2016) Circadian physiology of metabolism. *Science*, 354, 1008-1015.

Park, B.S., Tu, T.H., Lee, H., Jeong, D.Y., Yang, S., Lee, B.J. & Kim, J.G. (2019) Beta-Aminoisobutyric Acid Inhibits Hypothalamic Inflammation by Reversing Microglia Activation. *Cells*, 8, 1609.

Roberts, Lee D., Boström, P., O'Sullivan, John F., Schinzel, Robert T., Lewis, Gregory D., Dejam, A., Lee, Y.-K., Palma, Melinda J., Calhoun, S., Georgiadi, A., Chen, M.-H., Ramachandran, Vasan S., Larson, Martin G., Bouchard, C., Rankinen, T., Souza, Amanda L., Clish, Clary B., Wang, Thomas J., Estall, Jennifer L., Soukas, Alexander A., Cowan, Chad A., Spiegelman, Bruce M. & Gerszten, Robert E. (2014) β-Aminoisobutyric Acid Induces Browning of White Fat and Hepatic β-Oxidation and Is Inversely Correlated with Cardiometabolic Risk Factors. *Cell Metabolism*, 19, 96-108.

Roser, M.O.-O., E.; Ritchie, H. (2013) life expectancy. *OurWorldInData.org*, Online Resource.

Sato, S., Solanas, G., Peixoto, F.O., Bee, L., Symeonidi, A., Schmidt, M.S., Brenner, C., Masri, S., Benitah, S.A. & Sassone-Corsi, P. (2017) Circadian Reprogramming in the Liver Identifies Metabolic Pathways of Aging. *Cell*, 170, 664-677 e611.

Schilperoort, M., van den Berg, R., Bosmans, L.A., van Os, B.W., Dolle, M.E.T., Smits, N.A.M., Guichelaar, T., van Baarle, D., Koemans, L., Berbee, J.F.P., Deboer, T., Meijer, J.H., de Vries, M.R., Vreeken, D., van Gils, J.M., Willems van Dijk, K., van Kerkhof, L.W.M., Lutgens, E., Biermasz, N.R., Rensen, P.C.N. & Kooijman, S. (2020) Disruption of circadian rhythm by alternating light-dark cycles aggravates atherosclerosis development in APOE*3-Leiden.CETP mice. *Journal of Pineal Research*, 68, e12614.

Schmitt, E.E., Johnson, E.C., Yusifova, M. & Bruns, D.R. (2019) The renal molecular clock: broken by aging and restored by exercise. *American Journal of Physiology-Renal Physiology*, 317, F1087-F1093.

Srivastava, S. (2019) Emerging Insights into the Metabolic Alterations in Aging Using Metabolomics. *Metabolites*, 9, 301.

Tognini, P., Samad, M., Kinouchi, K., Liu, Y., Helbling, J.-C., Moisan, M.-P., Eckel-Mahan, K.L., Baldi, P. & Sassone-Corsi, P. (2020) Reshaping circadian metabolism in the suprachiasmatic nucleus and prefrontal cortex by nutritional challenge. *Proceedings of the National Academy of Sciences*, 117, 29904-29913.

Welz, P.-S. & Benitah, S.A. (2020) Molecular Connections Between Circadian Clocks and Aging. *Journal of Molecular Biology*, 432, 3661-3679.

Xin, H., Deng, F., Zhou, M., Huang, R., Ma, X., Tian, H., Tan, Y., Chen, X., Deng, D., Shui, G., Zhang, Z. & Li, M.-D. (2021) A multi-tissue multi-omics analysis reveals distinct kineztics in entrainment of diurnal transcriptomes by inverted feeding. *iScience*, 24, 102335.

Yang, J., Chen, T., Sun, L., Zhao, Z., Qi, X., Zhou, K., Cao, Y., Wang, X., Qiu, Y., Su, M., Zhao, A., Wang, P., Yang, P., Wu, J., Feng, G., He, L., Jia, W. & Wan, C. (2013) Potential metabolite markers of schizophrenia. *Molecular Psychiatry*, 18, 67-78.

Zierer, J., Menni, C., Kastenmüller, G. & Spector, T.D. (2015) Integration of 'omics' data in aging research: from biomarkers to systems biology. *Aging Cell*, 14, 933-944.

Supplemental material

Supplemental figures

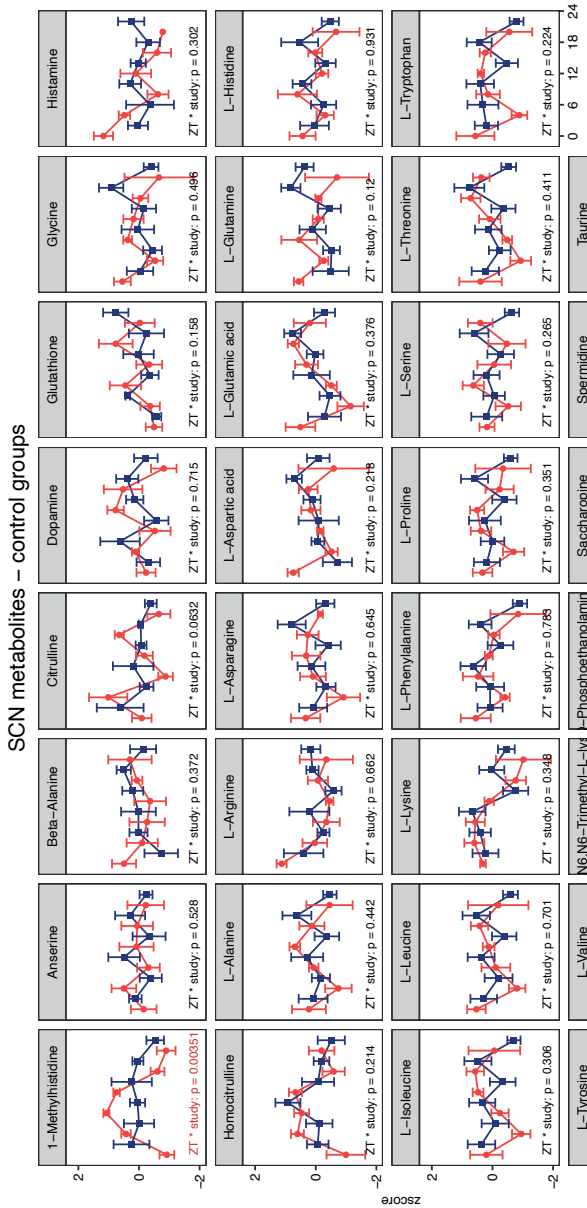

Figure S1. Comparison of data form control group (young mice) with previously published metabolomics analysis of SCN, liver and blood plasma. Data from the present study (blue) is compared with results from Dyar et al., 2018 (red). P-value of < 0.05 indicated significantly different temporal pattern.

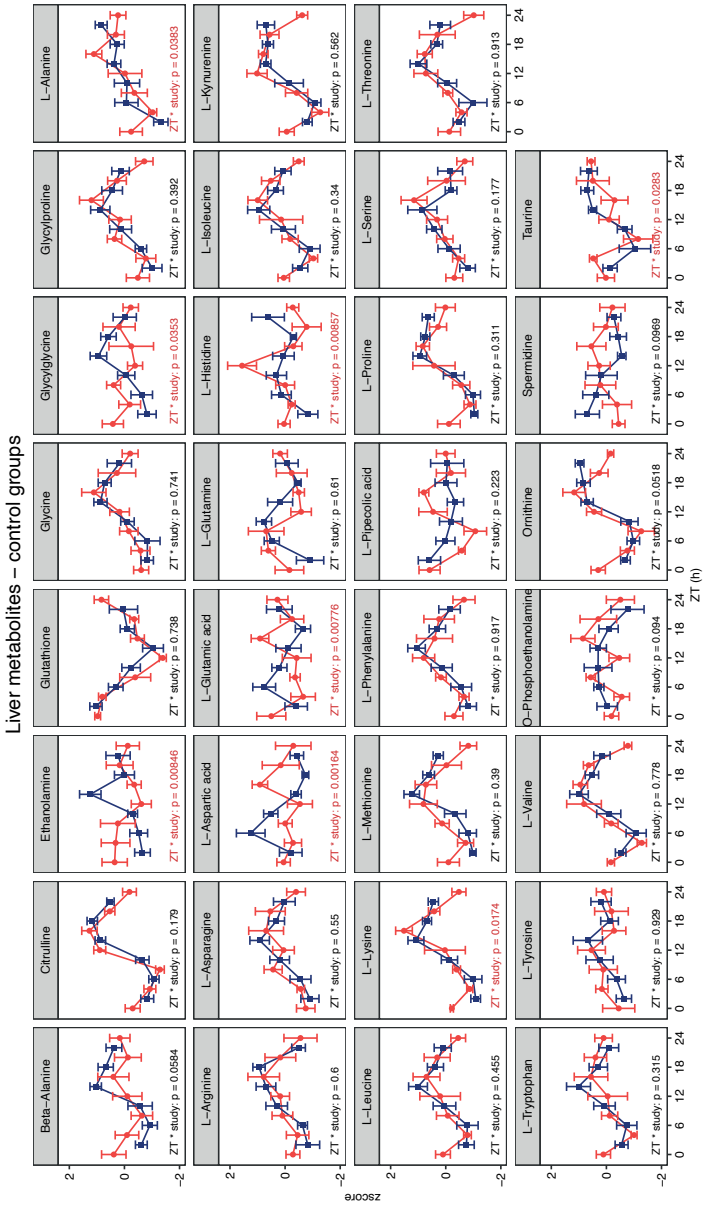

Figure S1. Continued

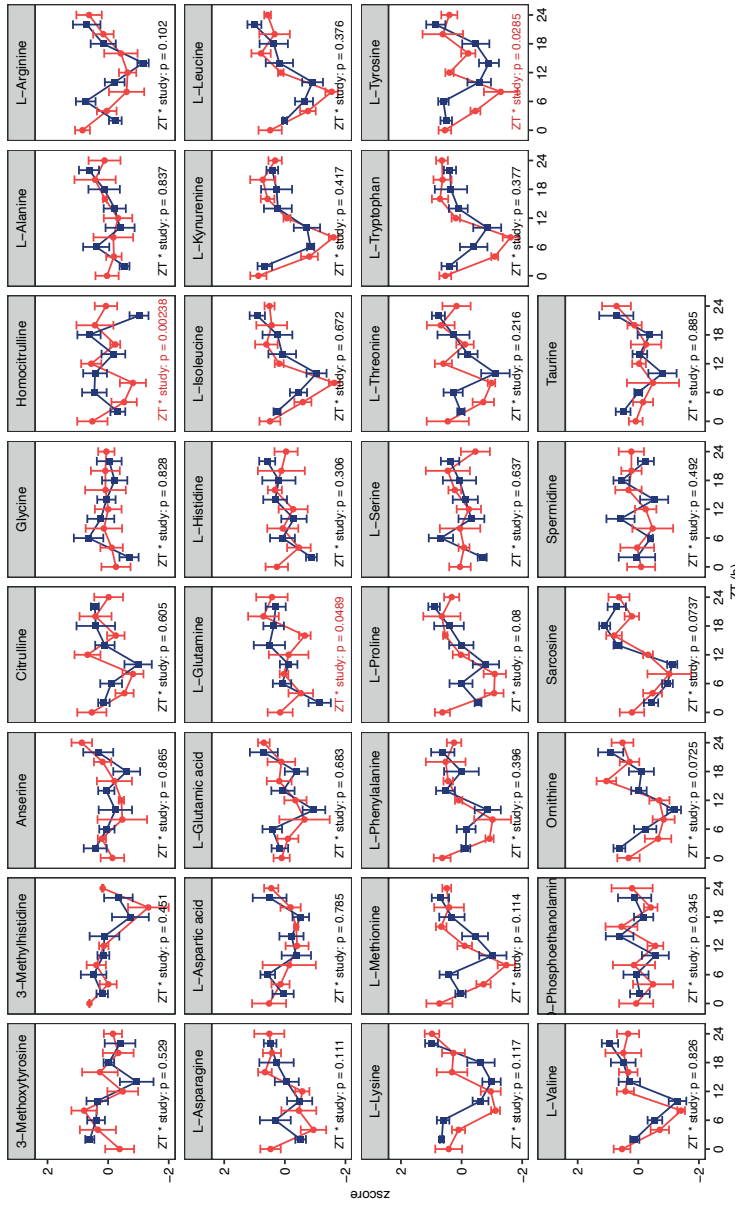

Figure S1. Continued

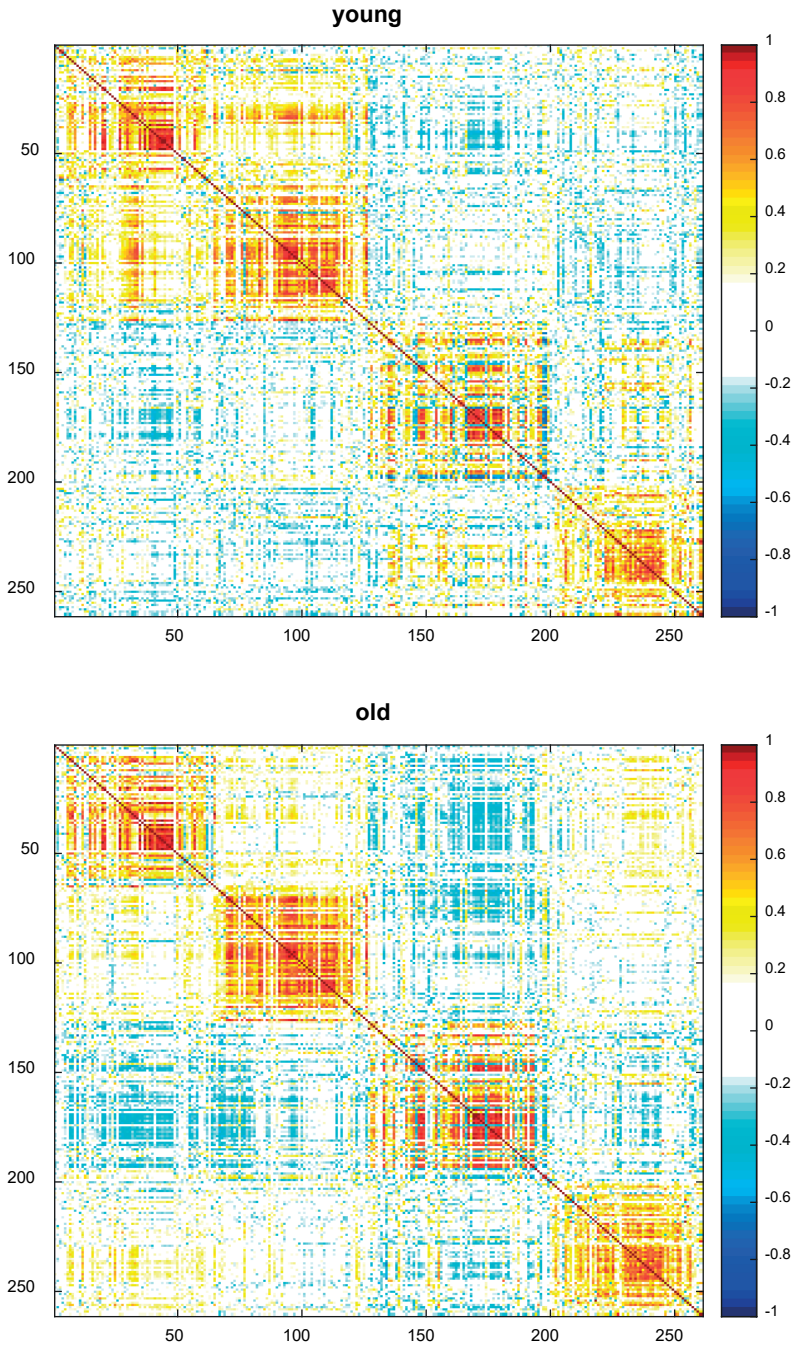

Figure S2. Correlation matrix for all metabolites in the four examined tissues from young and old mice. Color-code indicates spearman's rho correlation coefficient. Row/column: 1-66 SCN, 67-127 PVN, 128-200 liver, 201-261 plasma.